Brief communication: Potential of satellite optical imagery to monitor glacier surface flow velocity variability in the tropical Andes

Etienne Ducasse[1], Romain Millan[1], Jonas Kvist Andersen[2] and Antoine Rabatel[1]

[1]Univ. Grenoble Alpes, CNRS, IRD, INRAE, Grenoble-INP, IGE (UMR 5001), 38000 Grenoble, France

[2]Department of Geosciences and Natural Resource Management, University of Copenhagen, Copenhagen K, Denmark

Correspondence: Romain Millan (romain.millan@univ-grenoble-alpes.fr) and Antoine Rabatel (antoine.rabatel@univ-grenoble-alpes.fr)

Abstract

We present an analysis of glacier dynamics in mountain ranges of the tropical Andes of southern Peru and Bolivia using satellite data from 2013 to 2022. Despite the challenges posed by small-size glaciers, low velocities and high cloudiness during the monsoon, we map annually aggregated surface velocities and quantify the seasonal variability in the fastest parts of the glaciers. Limited trends are observed on the annual velocities over the last decade, but significant seasonal changes between the wet and the dry seasons are found, likely controlled by the seasonality in melt water production and the related changes in the hydrological conditions at the glacier-bedrock interface.

1. Introduction

Ice flow velocity is a critical variable characterizing the dynamics of glaciers and ice caps, serving as a valuable indicator of their response to climate change. Ice flow velocity is also of paramount importance as it enables to: (i) infer various other physical variables of glaciers such as ice thickness distribution, basal sliding or friction; (ii) quantify mass fluxes and loss through ice discharge into lakes or into the sea; and (iii) study glacial instability phenomena such as ice avalanches, glacier or ice shelves destabilizations (Gilbert et al., 2018; Millan et al., 2023; Jager et al., 2024). Until now, available observations of flow velocities for mountain glaciers (excluding ice caps) have been limited to large glaciers, temporally averaged (Millan et al., 2022), quantified at coarse spatial resolutions of hundreds of metres (GoLIVE, Scambos et al., 2016; ITS_LIVE, Gardner et al., 2024), or at local scale (Van Wyk de Vries et al., 2022). This directly impacts the study of small glacial features in regions such as the tropical Andes, which experience some of the highest mass losses (Hugonnet et al., 2023).

In the tropical Andes, many studies have been dedicated to surface-area or volume changes over the last decades-to-centuries (e.g., Hastenrath and Ames, 1995; Rabatel et al., 2005, 2013; Basantes-Serrano et al., 2022) and to surface mass balance processes and their relationships with climate conditions and particularly the ENSO (e.g., Kaser, 2001; Francou et al., 2003; Rabatel et al., 2013), but the spatio-temporal variability of glacier flow in the tropical region has never been explored in details. This leaves a significant knowledge gap in our understanding of glacier dynamics and their response to changes in surface processes, thermal regime or subglacial hydrology under tropical conditions, with direct consequences on ice flow modeling capacities. However, tropical glaciers pose greater challenges than other mountain regions because glaciers are much smaller (a few hundred metres wide), much slower (flow velocity typically <100 m.yr^{-1}) and in climate conditions that do not favour continuous optical satellite coverage; *e.g.*, high cloudiness during the monsoon season that typically spans from November-December to March-April in the Andes of Peru and Bolivia where our study is focused (*e.g.*, Rabatel et al., 2012; Autin et al., 2022).

Therefore, we propose to reconstruct and analyse, the evolution of the dynamics of glaciers located in tropical mountain ranges in the Andes of southern Peru and Bolivia from the years 2013 to the present, building on previous mapping from Millan et al. (2019, 2022). We explore the spatial and temporal variabilities of glacier flow at both decadal and seasonal scales, thus providing the first observations of glacier dynamics variability in a Tropics.

2. Methods

2.1. Ice velocity processing

The overall workflow we have developed to retrieve glacier surface flow velocity from satellite imagery has been fully described and validated on a large diversity of glaciers in the Andes, European Alps and New Zealand (Millan et al., 2019; Mouginot et al., 2023; Rabatel et al., 2023). Here we only present a short description of the four modules: (1) database creation and image preparation; (2) glacier surface displacement calculation; (3) data calibration; and (4) post-processing with data filtering and averaging to obtain glacier surface velocity maps.

The image preparation module automatically downloads Sentinel-2 and Landsat-8 ortho-rectified images and create pairs of images with repeat cycles ranging from 5 to 400 days, matching acquisitions in the same orbits for each satellite to minimize residual stereoscopic effects. Additionally, we enhance surface features using a Sobel filter on Sentinel-2's band #8 and the panchromatic band of Landsat-8. To derive glacier surface displacement, we calculate the standardized cross-correlation between two images within a pair (details on window size can be found in Millan et al., 2019 and Rabatel et al., 2023). We automatically calibrate glacier surface flow velocity using ice-free areas to mitigate potential biases arising from relative geometric distortions or geolocation errors between image pairs (see Millan et al., 2019). Our region of interest (RoI) is shown in Figure 1 and encompasses several glacierized cordilleras in the Andes of southern Peru and northern Bolivia. Glacier outlines are taken from the V6.0 of the Randolph Glacier Inventory (RGI Consortium, 2017). The RoI is divided into 159 geo-cubes distributed

throughout the study region and with an imprint of 250x250 pixels with a spatial resolution of 50 m. As made for the European Alps in Rabatel et al. (2023), this standardized dataset is stored on a common grid to facilitate the extraction of time series of the surface flow velocity or calculate time-averaged maps.

2.2. Annual maps production and seasonal signal extraction

For each geo-cube, a temporal pixel-by-pixel filtering is first performed based on different criteria described in Rabatel et al. (2023). Then, the filtered maps are aggregated into annual mosaics, which are spatially filtered following the procedure described in Rabatel et al. (2023). To aggregate the individual velocity measurements, we used the Ordinary Least Square (OLS), also called linear regression method (Mouginot et al., 2023). Unreliable pixels are flagged if they present a large variability after filtering, using a coefficient of variation above 75%, or if the standard deviation on the surface flow direction exceeds 2.5°. The trend is considered significant according to a Mann–Kendall test (Rabatel et al., 2023) and a mask is generated on this basis (Fig. 1B, D, F). The hypothesis of the presence of a monotonic trend in the time series is accepted with a p-value of the test is below 0.05. Finally, a spatial filtering on the trend map that uses a 5×5 median filter is applied. To extract the seasonal signal from time series data, we use a Locally Weighted Scatter-plot Smoothing (LOWESS) method. The principle is to perform regression on a certain number of points using a linear or quadratic function over a sliding window, the size of which is determined based on the availability of observation data (Derkacheva et al., 2020). This method is used to automatically determine the approximate dates of seasonal peaks from year to year. We only derived the LOWESS fit when we have a sufficient density of observations, more often during dry seasons after 2016 (Fig. 2).

3. Results

3.1. Overall description and decadal trend

Surface flow velocity maps reveal flow patterns on the smallest glacial features (*e.g.*, 1 km^2 on average), where this variable has been measured using medium-resolution satellites (10-15 meters pixel size) with global coverage. Generally, surface velocity rarely exceeds 50 m.yr^{-1}. However, locally, in the steepest parts of the glacier tongues, velocities can exceed 80 m.yr^{-1}, such as on Ausangate South Glacier (Cordillera Vilcanota, Peru) with velocities beyond 100 m.yr^{-1} (Fig. 1A), or the lower part of Ancohuma Glacier (Cordillera Real, Bolivia), the main tongue of Ancohuma West (Fig. 1C), or on the Chaupi Orco Noth-west Glacier located in the Cordillera Apolobamba at the border between Peru and Bolivia (Fig. 1E). We have evaluated our results by comparing the annually aggregated velocity values with annual *in situ* d-GNSS measurements of ablation stakes displacement located in the lower tongue of the Zongo Glacier in Bolivia where surface flow velocities range between 5 to 25 m.yr^{-1} (Réveillet et al., 2015). Such velocities are low and we are reaching the limits of the precision of satellite derived surface flow velocities (Millan et al., 2019). D-GNSS data are within the level of error of the annually aggregated data, with standard deviations ranging between 10-15 m.yr^{-1}. The scatter plot of this comparison can be found

in Figure S1. Nonetheless, the same kind of comparison was made in the Alps with a larger dataset of d-GNSS measurements made at locations where velocities reach up to 120 m.yr^{-1}, hence where the signal-to-noise ratio is more favorable for satellite derived velocities. In this region, we obtained a very high performance of satellite-derived glacier flow velocity with a root mean squared error of 10.5 m.yr^{-1} and a coefficient of determination of 0.92 (Rabatel et al., 2023).

In order to characterize decadal velocity trends, we analyze the regression coefficient values pixel by pixel (Fig. 1 B, D, F). We observe very low trends over the period 2013-2022, with values mostly ranging between -2 and +2 m.yr^{-2}. Some exceptions can be highlighted, notably with an increase in velocities exceeding 6 m.yr^{-2} on the Glacier Chaupi Orco North West (Fig. 1F) located on the Nevado Chaupi. On the detailed time series (Fig. 2, bottom), we shown that this glacier underwent a sudden "surge-type" acceleration in 2020-2022, to reach a maximum velocity on May 2022 at 160 m.yr^{-1}. In agreement with an unusual behavior, one can note that the surface velocities at Chaupi Orco are increasing during the dry period, *i.e.* between April-May and October 2021, when a large number of data are available giving confidence on this observation. At this period of the year, the velocity of the other glaciers is, on the contrary, seasonally decreasing. During about 18 months, the velocity on the glacier tongue continuously exceeded 100 m.yr^{-1}, which is more than twice the average of the period 2013-2020. Glacier Chaupi Orco North West is a lake-terminating glacier. On Figure S2, one can note: (1) the presence of numerous small icebergs during the event at the proglacial lake surface, contrasting with the years before and after the event, *i.e.* 2021 and 2024; (2) the widening of the glacier tongue; and (3) an almost disappearance of the debris-cover on both sides of the tongue. Although visual and qualitative, these elements go hand-to-hand with a strong increase in the ice flux. Glacier surge is a phenomenon quite unusual on tropical glaciers but that has already been mentioned on one of the glaciers on the Antisana Volcano in Ecuador (Basantes-Serrano et al., 2022).
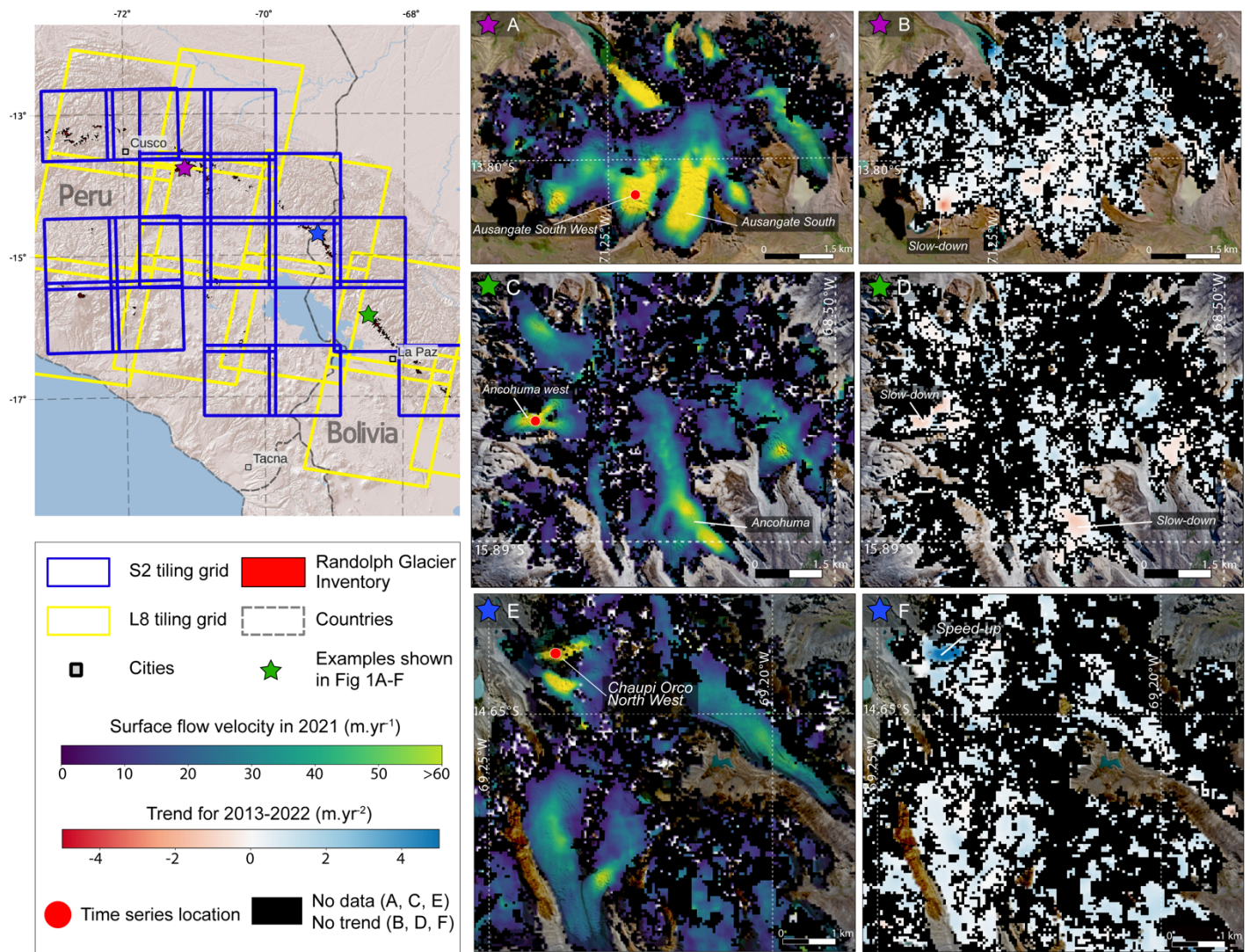
Figure 1: *Sentinel-2 and Landsat-8 tiles covering the glaciers in the tropical Andes of Southern Peru and Northern Bolivia considered for glacier surface flow velocity mapping. Inset boxes show the mapped ice flow velocities field for 2021 (left) and velocities trends for the 2013-2022 period (right), for three areas (colored stars): (A, B) Nevado Ausangate (C, D) Ancohuma region; (E, F) central part of Cordillera Apolobamba. Background maps for A-F is a cloudless mosaic of Sentinel-2 imagery.*

3.2. Seasonal changes in surface flow velocities

For the glaciers presented in Figure 2, we observe a strong seasonality in the surface velocities, particularly between the wet season (from approx. November to March) and the dry season (from approx. April to October). For the Ancohuma West Glacier, the surface flow velocity decreases from 120 m.yr⁻¹

in May to 20 m.yr⁻¹ in September, representing a reduction of over 80%. Similar variations are observed throughout the study area, with, for example, a decrease in surface velocities of 60% for the glaciers located on the southern flank of the Ausangate summit (see Fig. 1). This seasonality repeats year after year and is observed for a large number of other glaciers in the RoI (not shown). However, it is important to note that the glaciers of Ancohuma and Ausangate are among those where it is possible to observe the beginning of the acceleration marking the transition to the wet season in 2021 and 2022, generally occurring in September-October (Fig. 2).
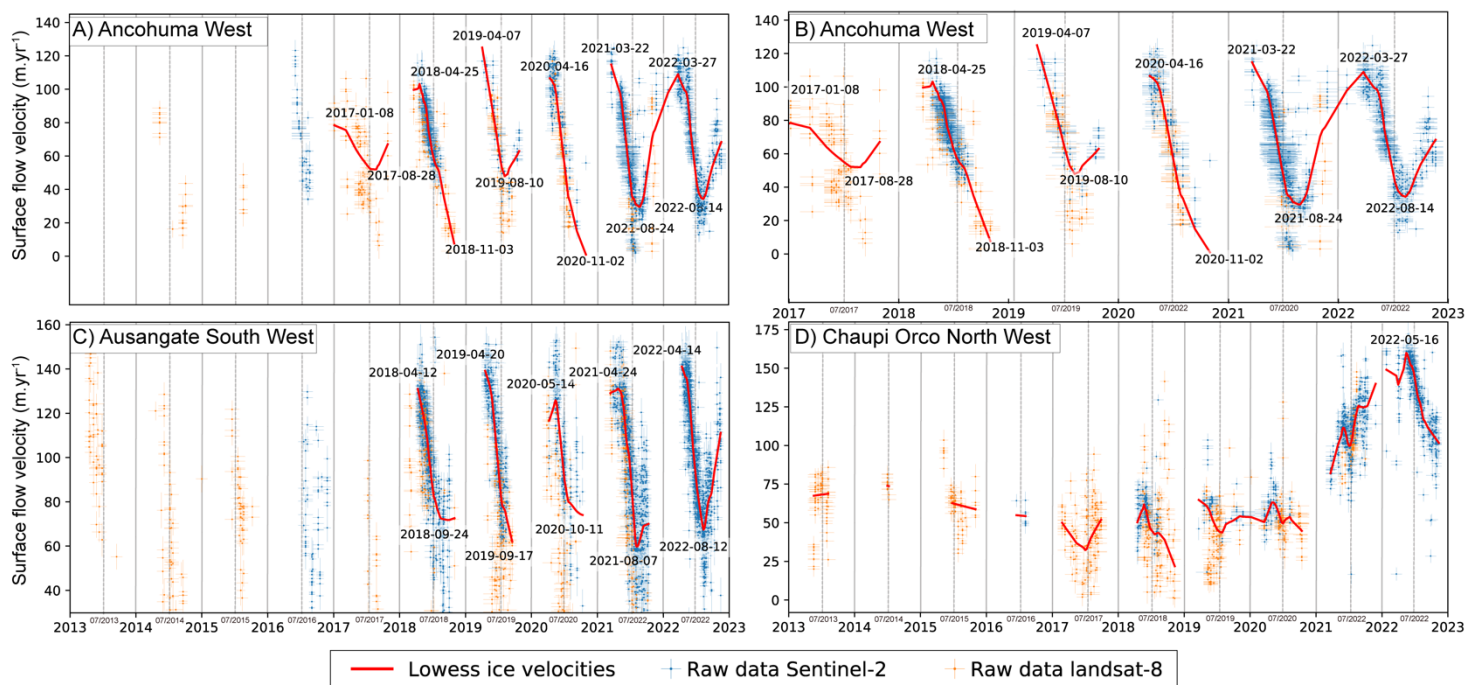
Figure 2: *Time series of surface flow velocities on selected glaciers shown in Figure 1 (red dots in Fig. 1A, C and E). A glacier tongue on the western side of Ancohuma (called Ancohuma West) between 2013 and 2022 (top left), and zoom into the 2017-2022 period (top right). A glacier located in the southwestern side of Ausangate (called Ancohuma South West, bottom left) and one located on the northwestern side of Chaupi Orco (bottom right). The velocity is calculated on a 3x3 pixels window size.*

4. Discussion

For the first time, we highlight the spatio-temporal variability of glacier dynamics in the tropical Andes. In addition to the decadal changes, we also identify the existence of a seasonal cycle in velocities between the wet and dry seasons that has never been observed before (Fig. 2). We measure a unique dynamical behaviour with significant velocity variations over scales ranging from 4 to 5 months, with reductions of up to 80% (Fig. 2). It is worth noting that we only observe the glacier surface flow velocities over the period between March-April to October-November (*i.e.* between the end of the wet season and beginning

of the next one). Indeed, the very high cloudiness of the monsoon regime affecting South America during the wet season (*i.e.* between November-December to March-April) strongly limits the use of optical satellite imagery.

155 Therefore, there are uncertainties concerning the timing and magnitude of maximum velocity peak, which may occur earlier in the wet season. The use of radar interferometry would be required to measure these flow changes more accurately, specifically for small moving regions (*e.g.*, on ice cap) and during the wet season. However, this remains very challenging due to the pronounced topography (shadowing/layover), climatic conditions favouring temporal loss of coherence (high precipitation rates and surface melting).

160 These difficulties in recovering phase coherence are illustrated on interferograms examples provided in Figures S3 and S4.

The strong seasonal cycle observed in the glacier surface velocity data can be explained in the light of the glaciological regime of the tropical glaciers. On the basis of 27 years of continuous monthly measurements of the surface mass balance of Zongo Glacier (Bolivian Cordillera Real), Autin et al. (2022)

165 have shown that the surface mass balance is strongly negative during the transition period between and dry and the wet seasons, *i.e.* from September to December with the most negative values reached in November. Melting remains high during the wet season counterbalancing in the ablation area of the glacier the intense snowfalls occurring during the monsoon. From April to August, ablation is limited and largely occurs through sublimation thus strongly limiting the water production. Therefore, the progressive

170 increase in melting at the glacier surface from September to November leads to a strong water inflow inside and at the bedrock interface of the glacier when the drainage system is particularly inefficient after the dry season. This leads to increasing water pressure and progressively increasing basal sliding which results in an increase in surface flow velocities as seen in Figure 2 for Ausangate and Ancohuma glaciers, particularly for the last two years of observation. Then, the strong surface melt rates during the wet season

175 maintain high meltwater discharges that promote the development of efficient subglacial drainage networks. At the end of the wet season (*i.e.* in March-April) decreasing melt rates at the glacier surface limit the water discharge thus explaining the large slowdown in glacier flow velocities. Even if the glaciological regime differs in the tropics in comparison to the mid-latitudes, such seasonal pattern is consistent with what has been described by Gilbert et al. (2022) on the Argentière Glacier in the French

180 Alps.

The changes in glacier flow in the Andes are close to the limits of what can be accurately measured using Landsat-8 and Sentinel-2 satellites (Millan et al., 2019). This is due to the very small size of the glaciers, as well as their very slow flow velocities, typically lower than 50 m.yr^{-1}. High-resolution measurements of glacier flow (*e.g.*, SPOT, Pléiades), as well as continuous field measurements (*e.g.*, d-GNSS) would

185 be useful for strengthening the analysis presented here. However, our study shed light on previously unexplored dynamics processes in tropical glaciers with implications for understanding their dynamical response to changes in surface melt and sub-glacial hydrology.

Finally, it should be noted that glaciers in the mountain ranges studied here do not present a debris cover. In other cordilleras of the tropical Andes, such as Peru's Cordillera Blanca, debris-covered glaciers are

190 more numerous, and in situ velocity measurements have been made on some of them (e.g., Hubbard and Clemmens, 2008). Although these debris-covered glacier tongues have low velocities, generally less than

a few tens of metres per year, their surface texture (linked to the debris) and temporal persistence mean that correlation algorithms using long temporal baselines (e.g., a year or more) can allow to retrieve consistent velocity values, as shown by Cusicanqui et al. (2024) using Landsat data on rock glaciers in
195 Chile.

Author contribution

R.M, A.R designed the study. R.M, E.D and J.A developed the code, processed and analyzed the data. E.D prepared the manuscript with contributions from all co-authors.

Competing interests

200 The authors declare that they have no conflict of interest.

Acknowledgments

This work was performed at the *Institut des Géosciences de l'Environnement* and at the University of Copenhagen. E.D., R.M. and A.R. acknowledge funding from the OSUG LabEx OSUG@2020 (*Investissement d'Avenir*, ANR-10-LABX-56). J.A. acknowledges funding from the Villum Foundation
205 (Villum Young Investigator grant no. 29456). We acknowledge the *Service National d'Observation* GLACIOCLIM (UGA-OSUG, CNRS-INSU, IRD, INRAE, Météo-France, IPEV) and its counterpart in Bolivia (UMSA-IGEMA, Dr. Alvaro Soruco) for the long-term monitoring of Zongo Glacier. This work is dedicated to Jérémie Mouginot, co-PI of the LabEx project, who passed away in September 2022.

Data and code availability

210 Annual surface flow velocity maps for 2013-2022, along with velocity direction, trends and error maps are available at https://doi.org/10.57745/OJBTSE

References

1. Autin, P., Sicart, J. E., Rabatel, A., Soruco, A., and Hock, R.: Climate controls on the interseasonal
215 and interannual variability of the surface mass and energy balances of a tropical glacier (Zongo Glacier, Bolivia, 16° S): new insights from the multi-year application of a distributed energy balance model. J. Geophys. Res.: Atmospheres, 127(7), e2021JD035410. https://doi.org/10.1029/2021JD035410, 2022.

2. Basantes-Serrano, R., Rabatel, A., Francou, B., Vincent, C., Soruco, A., Condom, T., and Ruíz, J.C.: New insights into the decadal variability in glacier volume of a tropical ice cap, Antisana (0° 29′ S, 78° 09′ W), explained by the morpho-topographic and climatic context. The Cryosphere, 16(11), 4659-4677. https://doi.org/10.5194/tc-16-4659-2022, 2022.

3. Cusicanqui, D., Lacroix, P., Bodin, X., Robson, B.A., Kääb, A., and MacDonell, S.: Detection and reconstruction of rock glaciers kinematic over 24 years (2000–2024) from Landsat imagery, EGUsphere [preprint], https://doi.org/10.5194/egusphere-2024-2393, 2024.

4. Derkacheva, A., Mouginot, J., Millan, R., Maier, N., and Gillet-Chaulet, F.: Data reduction using statistical and regression approaches for ice velocity derived by Landsat-8, Sentinel-1 and Sentinel-2, Remote Sensing, 12, 1935, https://doi.org/10.3390/rs12121935, 2020.

5. Francou, B., Vuille, M., Wagnon, P., Mendoza, J., and Sicart, J.E.: Tropical climate change recorded by a glacier in the central Andes during the last decades of the twentieth century: Chacaltaya, Bolivia, 16 S, J. Geophys. Res.: Atmos., 108(D5), https://doi.org/10.1029/2002JD002959, 2003.

6. Gardner, A.S., Fahnestock M.A., and Scambos T.A.: MEaSUREs ITS_LIVE Landsat image-pair glacier and ice sheet surface velocities: Version 1. Data archived at National Snow and Ice Data Center. https://doi.org/10.5067/IMR9D3PEI28U, 2024.

7. Gilbert, A., Leinss, S., Kargel, J., Kääb, A., Gascoin, S., Leonard, G., Berthier, E., Karki, A., and Yao, T.: Mechanisms leading to the 2016 giant twin glacier collapses, Aru Range, Tibet, The Cryosphere, 12, 2883–2900, https://doi.org/10.5194/tc-12-2883-2018, 2018.

8. Gilbert, A., Gimbert, F., Thøgersen, K., Schuler, T. V., and Kääb, A.: A consistent framework for coupling basal friction with subglacial hydrology on hard-bedded glaciers, Geophys. Res. Lett., 49(13), e2021GL097507. https://doi.org/10.1029/2021GL097507, 2022.

9. Hastenrath, S., and Ames, A.: Recession of Yanamarey glacier in Cordillera Blanca, Peru, during the 20th century, J. Glaciol., 41(137), 191-196, https://doi.org/10.3189/S0022143000017883, 1995.

10. Hubbard, B., and Clemmens, S.: Recent high-resolution surface velocities and elevation change at a high-altitude, debris-covered glacier: Chacraraju, Peru, J. Glaciol., 54(186), 479-486, https://doi.org/10.3189/002214308785837057, 2008.

11. Hugonnet, R., Millan, R., Mouginot, J., Rabatel, A., and Berthier, E.: Un atlas mondial pour caractériser la réponse des glaciers au changement climatique. La Météorologie, 120, 037. https://doi.org/10.37053/lameteorologie-2023-0015, 2023.

12. Jager, E., Gillet-Chaulet, F., Mouginot, J., and Millan, R.: Validating ensemble historical simulations of Upernavik Isstrøm (1985–2019) using observations of surface velocity and elevation, J. Glaciol., 1–18, https://doi.org/10.1017/jog.2024.10, 2024.

13. Kaser, G.: Glacier-climate interaction at low latitudes, J. Glaciol., 47(157), 195-204, https://doi.org/10.3189/172756501781832296, 2001.

14. Millan, R., Mouginot, J., Rabatel, A., Jeong, S., Cusicanqui, D., Derkacheva, A., and Chekki, M.: Mapping surface flow velocity of glaciers at regional scale using a multiple sensors approach, Remote Sensing, 11, 2498, https://doi.org/10.3390/rs11212498, 2019.

15. Millan, R., Mouginot, J., Derkacheva, A., Rignot, E., Milillo, P., Ciraci, E., Dini, L., and Bjørk, A.: Ongoing grounding line retreat and fracturing initiated at the Petermann Glacier ice shelf, Greenland, after 2016, The Cryosphere, 16, 3021–3031, https://doi.org/10.5194/tc-16-3021-2022, 2022.

16. Millan, R., Jager, E., Mouginot, J., Wood, M.H., Larsen, S.H., Mathiot, P., Jourdain, N.C., and Bjørk, A.: Rapid disintegration and weakening of ice shelves in North Greenland, Nat. Commun., 14, 6914, https://doi.org/10.1038/s41467-023-42198-2, 2023.

17. Mouginot, J., Rabatel, A., Ducasse, E., and Millan, R.: Optimization of cross correlation algorithm for annual mapping of alpine glacier flow velocities; application to Sentinel-2, IEEE Trans. Geosci. Remote Sensing, 61, 1–12, https://doi.org/10.1109/TGRS.2022.3223259, 2023.

18. Rabatel, A., Jomelli, V., Naveau, P., Francou, B., and Grancher, D.: Dating of Little Ice Age glacier fluctuations in the tropical Andes: Charquini glaciers, Bolivia, 16 S, Comptes Rendus Géoscience, 337(15), 1311-1322, https://doi.org/10.1016/j.crte.2005.07.009, 2005.

19. Rabatel, A., Bermejo, A., Loarte, E., Soruco, A., Gomez, J., Leonardini, G., Vincent, C., and Sicart, J.E.: Can the snowline be used as an indicator of the equilibrium line and mass balance for glaciers in the outer tropics?, J. Glaciol., 58, 1027–1036, https://doi.org/10.3189/2012JoG12J027, 2012.

20. Rabatel, A., Francou, B., Soruco, A., Gomez, J., Cáceres, B., Ceballos, J. L., Basantes, R., Vuille, M., Sicart, J.-E., Huggel, C., Scheel, M., Lejeune, Y., Arnaud, Y., Collet, M., Condom, T., Consoli, G., Favier, V., Jomelli, V., Galarraga, R., Ginot, P., Maisincho, L., Mendoza, J., Ménégoz, M., Ramirez, E., Ribstein, P., Suarez, W., Villacis, M., and Wagnon, P.: Current state of glaciers in the tropical Andes: a multi-century perspective on glacier evolution and climate change, The Cryosphere, 7, 81–102, https://doi.org/10.5194/tc-7-81-2013, 2013.

21. Rabatel, A., Ducasse, E., Millan, R., and Mouginot, J.: Satellite-derived annual glacier surface flow velocity products for the European Alps, 2015–2021, Data, 8(4), 66. https://doi.org/10.3390/data8040066, 2023.

22. Réveillet, M., Rabatel, A., Gillet-Chaulet, F., Soruco, A. : Simulations of changes to Glaciar Zongo, Bolivia (16°S), over the 21st century using a 3-D full-Stokes model and CMIP5 climate projections, A. Glaciol., 56(70), 89-97, https://doi.org/10.3189/2015AoG70A113, 2015.

23. RGI Consortium: Randolph Glacier Inventory – A Dataset of Global Glacier Outlines: Version 6.0: Technical Report, Global Land Ice Measurements from Space., https://doi.org/10.7265/N5-RGI-60, 2017.

24. Scambos, T., M. Fahnestock, T. Moon, A. Gardner, and M. Klinger. 2016. Global land ice velocity extraction from Landsat 8 (GoLIVE), Version 1. Boulder, Colorado USA. NASA National Snow and Ice Data Center Distributed Active Archive Center. https://doi.org/10.7265/N5ZP442B

25. Van Wyk de Vries, M., Carchipulla-Morales, D., Wickert, A.D., and Minaya, V.G.: Glacier thickness and ice volume of the Northern Andes, Sci. Data, 9, 342, https://doi.org/10.1038/s41597-022-01446-8, 2022.